TU/e EINDHOVEN UNIVERSITY OF TECHNOLOGY

Thermal and plasma enhanced atomic layer deposition of Al2O3on GaAs substrates

Citation for published version (APA):
Sioncke, S., Delabie, A., Brammertz, G., Conard, T., Franquet, A., Caymax, M., Urbanczyk, A. J., Heyns, M. M., Meuris, M., Hemmen, van, J. L., Keuning, W., & Kessels, W. M. M. (2009). Thermal and plasma enhanced atomic layer deposition of Al2O3on GaAs substrates. *Journal of the Electrochemical Society*, *156*(4), H255-H262. https://doi.org/10.1149/1.3076143

DOI:
10.1149/1.3076143

Document status and date:
Published: 01/01/2009

Document Version:
Publisher's PDF, also known as Version of Record (includes final page, issue and volume numbers)

Please check the document version of this publication:

• A submitted manuscript is the version of the article upon submission and before peer-review. There can be important differences between the submitted version and the official published version of record. People interested in the research are advised to contact the author for the final version of the publication, or visit the DOI to the publisher's website.
• The final author version and the galley proof are versions of the publication after peer review.
• The final published version features the final layout of the paper including the volume, issue and page numbers.

Link to publication

General rights
Copyright and moral rights for the publications made accessible in the public portal are retained by the authors and/or other copyright owners and it is a condition of accessing publications that users recognise and abide by the legal requirements associated with these rights.

• Users may download and print one copy of any publication from the public portal for the purpose of private study or research.
• You may not further distribute the material or use it for any profit-making activity or commercial gain
• You may freely distribute the URL identifying the publication in the public portal.

If the publication is distributed under the terms of Article 25fa of the Dutch Copyright Act, indicated by the "Taverne" license above, please follow below link for the End User Agreement:

www.tue.nl/taverne

Take down policy
If you believe that this document breaches copyright please contact us at:

openaccess@tue.nl

providing details and we will investigate your claim.

Download date: 16. Nov. 2023

Journal of The Electrochemical Society, **156** (4) H255-H262 (2009)
0013-4651/2009/156(4)/H255/8/$23.00 © The Electrochemical Society

Thermal and Plasma Enhanced Atomic Layer Deposition of Al_2O_3 on GaAs Substrates

Sonja Sioncke,[a,*,z] Annelies Delabie,[a,*] Guy Brammertz,[a,*] Thierry Conard,[a] Alexis Franquet,[a] Matty Caymax,[a,*] Adam Urbanzcyk,[a] Marc Heyns,[a,c] Marc Meuris,[a] J. L. van Hemmen,[b] W. Keuning,[b] and W. M. M. Kessels[b,*]

[a]*IMEC, B-3001 Leuven, Belgium*
[b]*Department of Applied Physics, Eindhoven University of Technology, 5600 MB Eindhoven, The Netherlands*
[c]*Department of Metallurgy and Materials Engineering, Katholieke Universiteit Leuven, Leuven, Belgium*

A good dielectric layer on the GaAs substrate is one of the critical issues to be solved for introducing GaAs as a candidate to replace Si in semiconductor processing. In literature, promising results have been shown for Al_2O_3 on GaAs substrates. Therefore, atomic layer deposition (ALD) of Al_2O_3 has been studied on GaAs substrates. We have been investigating the influence of the ALD process (thermal vs plasma-enhanced ALD) as well as the influence of the starting surface (no clean vs partial removal of the native oxide). Ellipsometry and total X-ray reflection fluorescence were applied to study the growth of the ALD layers. Angle-resolved X-ray photoelectron spectroscopy was used to determine the composition of the interlayer. Both processes were shown to be roughly independent of the starting surface with a minor dependence for the thermal ALD. Thermally deposited ALD layers exhibited better electrical characteristics based on capacitance measurements. This could be linked to the thinner interlayer observed for thermally deposited Al_2O_3. However, the Fermi level was not unpinned in all cases, suggesting that more work needs to be done for passivating the interface between GaAs and the high-*k* layer.
© 2009 The Electrochemical Society. [DOI: 10.1149/1.3076143] All rights reserved.

Manuscript submitted September 2, 2008; revised manuscript received November 13, 2008. Published February 5, 2009.

Si has been the dominant material in the semiconductor industry for several decades. Approaching the 22 nm node is forcing researchers to transfer from Si to other channel materials with inherent higher carrier mobility. For p-channel metal-oxide-semiconductor (pMOS), Ge is a possible candidate. Recent results on short-channel Ge pMOS have already demonstrated the high performance of Ge.[1] For nMOS applications, III/V compounds appear to be suitable candidates because of their high electron mobility. However, when introducing new materials, several topics have to be addressed before these materials can be introduced in cMOS processing.

One of the most challenging topics is the passivation of the interface between the channel material and the gate dielectric. The aim is to develop an interlayer that is as thin as possible, that removes the dangling bonds of the channel material, and that acts as an ideal starting surface for high-*k* deposition. Therefore, surface preparation and the choice of atomic layer deposition (ALD) process are critical.

Two-dimensional (2D) growth of ALD layers is preferred as layer closure is achieved faster for a 2D growth compared to an island-growth mechanism. Therefore, it is possible to make thin layers of good quality with a 2D growth process, which is important for downscaling. It has been established that the starting surface for ALD growth should have sufficient nucleation sites in order to achieve a 2D growth. Several studies have been carried out showing the dependence on the starting surface for HfO_2/H_2O ALD on Si substrates.[2-8] The reactivity of the starting surface can play a major role, but changing the reactivity of the precursors can be as important. For example, changing the alkylamino-hafnium precursors can lead to a more 2D growth mechanism.[9]

On III/V compounds, it has been claimed that Al_2O_3 ALD layers exhibit promising electrical properties.[10-12] Knowledge of the ALD of Al_2O_3 using trimethyl aluminum, [TMA = $Al(CH_3)_3$] as a metal precursor and H_2O as an oxidant has already been widely established,[13] and this process is referred to as thermal ALD. In this process, the TMA chemisorbs at the reactive hydroxyl sites (–OH) present on the substrate. Second, the ligands of the chemisorbed $Al(CH_3)_3$ are exchanged by hydroxyl groups by the reaction with H_2O, leaving Al_2O_3 on the surface and restoring the reactive –OH sites at the surface. However, O_2 plasmas are also used as an alternative oxidant. The same mechanism as described for the thermal ALD process takes place. However, in this case a combustion-like process removes the organic ligands. The O_2 plasma is an efficient oxidant. As a result, the deposition process is less dependent on the starting surface. Moreover, in the literature plasma-enhanced (PE) ALD has been reported to form stoichiometric $GaAsO_x$, which could form a possible passivation layer.[14] In this paper, the aim is to find a process for Al_2O_3 deposition on GaAs which results in high-quality ALD layers with good electrical behavior. Therefore, both thermal and PE ALD have been investigated for Al_2O_3 deposition on GaAs. The influence of the starting surface is studied for both ALD processes. Several wet-cleaning chemistries are screened, and thermal ALD deposition is compared to remote PE ALD deposition of Al_2O_3.

Experimental

TMA was used as the metal precursor in both ALD processes. For the thermal ALD processes, H_2O was used as an oxidant. Al_2O_3 was deposited at a temperature of 300°C and a pressure of 1 Torr. In the PE ALD process, O_2 plasma was used as an oxidant. The PE ALD studied here was a remote-plasma ALD, where plasma creation takes place remotely from the substrate but with the plasma species being present at the substrate. Also, for the PE ALD process, the Al_2O_3 was deposited at 300°C and a pressure of 15 mTorr. Before deposition, the sample was heated for 3 min in argon. Thermal ALD processes were performed in an ASM Pulsar[d] 2000 hot-wall cross-flow ALD reactor. The PE ALD was carried out with an Oxford Instruments FlexAL ALD tool.[15] The FlexAL reactor is equipped with an in situ spectroscopic ellipsometer (J. A. Woollam M-2000D, 193–1000 nm wavelength range), which makes it possible to monitor the growth of the Al_2O_3 layer during deposition. In order to determine the oxide thickness, a three-layer model is used assuming an Al_2O_3 and GaAs-oxide layer on top of bulk GaAs. For studying the thermal ALD process, only ex situ ellipsometry (plasmos) was available, operating at a wavelength of 633 nm. Also, only a two-layer model is used, assuming an Al_2O_3 oxide on top of the GaAs bulk. This means that the interfacial oxide is basically included in the Al_2O_3 layer. When comparing both ALD processes directly, ex situ measurements at room temperature are reported.

* Electrochemical Society Active Member.
z E-mail: sioncke@imec.be

[d] Pulsar is a trademark of ASM International.

Downloaded 11 May 2009 to 131.155.151.77. Redistribution subject to ECS license or copyright; see http://www.ecsdl.org/terms_use.jsp

Table I. Percentage of As- and Ga-oxides before Al_2O_3 deposition measured by AR-XPS. In the third column, the thickness of the GaAs oxide before Al_2O_3 deposition is determined by in situ SE. In the last column, the intercept of the growth curve is determined by in situ SE after 20 cycles of Al_2O_3 deposition by PE ALD. The intercept can be used as a measure for the increase in the GaAs-oxide thickness after deposition.

	% AsOx No Al_2O_3	% GaOx No Al_2O_3	d GaAsOx (nm) In situ SE, no Al_2O_3	d GaAsOx (nm) Intercept in situ SE, $+Al_2O_3$
No clean	7.68	6.74	1.70	1.80
HCl/DIW (1/10)	2.86	6.29	1.39	1.66
HF/DIW (1/10)	5.95	2.55	1.19	1.57
HBr/DIW (1/10)	0	4.89	1.01	1.38
$(NH_4)_2S$ 25 wt %	0	2.13	0.82	1.16
HCl_{conc}	1.73	2.18	—	—

To determine the Al content on the GaAs wafers, total X-ray reflection fluorescence (TXRF, FEI-Atomika 8300 W system) was used.

X-ray photoelectron spectroscopy (XPS) was performed on a Theta 300 system from Thermo Instruments in a parallel-angle resolved mode using monochromatized Al Kα radiation.

Time of flight-secondary ion mass spectrometry (TOF-SIMS) depth profiles were measured with an IONTOF IV instrument. Both positive and negative ion profiles were measured in the dual-ion-beam setup with a Ga (15 keV) gun for analysis and a Xe (350 eV) gun for sputtering. Atomic force microscopy (AFM) was used to determine the roughness of the deposited layers. A nanoscope IVa Dimension 3000 was used in tapping mode. Scan areas were 2 × 2 μm.

The substrates used were 50 mm p-type, Zn-doped wafers. Processing was done by means of pocket wafer processing. As the incoming GaAs wafers were highly contaminated with metals, the GaAs substrates received a sulfuric peroxide mixture (SPM = H_2SO_4/H_2O_2) clean. After this clean, the wafers were stored before further usage. During storage time, regrowth of the native oxide could be observed by ellipsometry. For all the wafers used in the reported experiments, a complete regrowth of ~1.7 nm of the native oxide could be seen. Therefore, we refer to these wafers as uncleaned wafers, although an SPM clean was carried out on each wafer. The influence of several cleaning chemistries on the growth mode was studied. To avoid regrowth of the native oxide, the time between the clean and the oxide deposition was minimized to less than ~10 min. In the case of the PE ALD, several starting surfaces were studied. "No clean" refers to a surface with a native oxide. The cleaning chemistries considered are diluted HCl (3.7 wt %), diluted HF (4.8 wt %), diluted HBr (4.9 wt %), and $(NH_4)_2S$ (25 wt %). For the HCl, HF, and HBr clean, a 5 min dip was performed. Immediately after the clean, the wafers were blown dry with a N_2 gun. The dip time for the $(NH_4)_2S$ clean was 0.5 min and was followed by a 1 min water rinse and dried with a N_2 gun. For the thermal ALD, only two starting surfaces were studied, no clean and concentrated HCl (37%). Again, a 5 min dip was performed, followed by a N_2 blow dry.

In order to evaluate interface quality through electrical measurements, simple metal-oxide-semiconductor (MOS) capacitors were fabricated on the samples. On the front side of the wafers, 50 nm thick Pt dots of different sizes were deposited through evaporation. AuZn/Au was used as the back-side ohmic contact. A forming gas anneal at 380°C was performed after the deposition for contact formation. The methods used for characterization of the interfaces include quasi-static and high-frequency capacitance–voltage (*C-V*). Capacitance dispersion in accumulation was also investigated. All of the quasi-static measurements were performed with an HP 4156C semiconductor parameter analyzer. As all of the samples showed signs of large slow-state populations, long integration times were used, which resulted in effective sweep rates of 3 mV/s. The quasi-static *C-V* curves were used to extract oxide capacitance and to estimate surface-potential variation with the Berglund method.[16] High-frequency *C-V* was done using an HP4284 LCR meter. Also, in this case, large integration times and slow sweep speeds were used; nevertheless hysteresis was observed. Investigated samples showed different amounts of frequency dispersion of the capacitance value due to interface states. Series resistance can also cause frequency dispersion; however, this effect is qualitatively different and depends on the size of the device under test, whereas the frequency dispersion caused by interface states is completely independent of device size.[17]

Results and Discussion

Starting surface.— XPS and in situ spectroscopic ellipsometry (SE) were used to determine the oxide thickness before Al_2O_3 deposition. The percentage of As- and Ga oxides determined by XPS are presented in Table I, and an overlay plot of the As 3d and Ga 3d is shown in Fig. 1. None of the pretreatments removes all the native oxides. However, the native oxide is thinned in all cases. The As oxides can be completely removed, in contrast to the Ga oxides. HBr and $(NH_4)_2S$ remove the As oxides. The lowest content of Ga oxides is found for the HCl_{conc} and the $(NH_4)_2S$ treatments. However, the presence of Ga–S instead of Ga–O cannot be excluded (binding energy shifts in XPS: Ga_2O_3 = 1.4 eV, Ga_2O = 0.7 eV, GaS = 0.7 eV). The difference in shifts in binding energy is so small between both chemical bounds that making the distinction is not trivial.[18,19] As a result, the shoulder in XPS at 0.7 eV could be attributed to a Ga–S or Ga–O bound. To conclude, $(NH_4)_2S$ is the most effective pretreatment for removing the native oxide even when assigning the peak shift observed in the Ga 3d peak to a Ga–O bound. Table I also shows the thickness of the GaAs oxide deter-

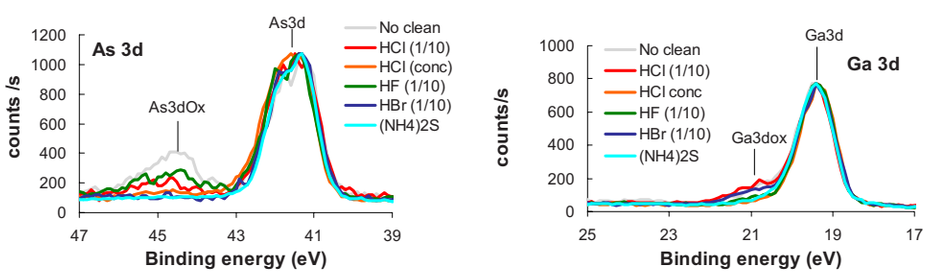

Figure 1. (Color online) As 3d and Ga 3d XPS spectra of the GaAs substrate for several cleaning chemistries at a detection angle of 28.88°.

Downloaded 11 May 2009 to 131.155.151.77. Redistribution subject to ECS license or copyright; see http://www.ecsdl.org/terms_use.jsp

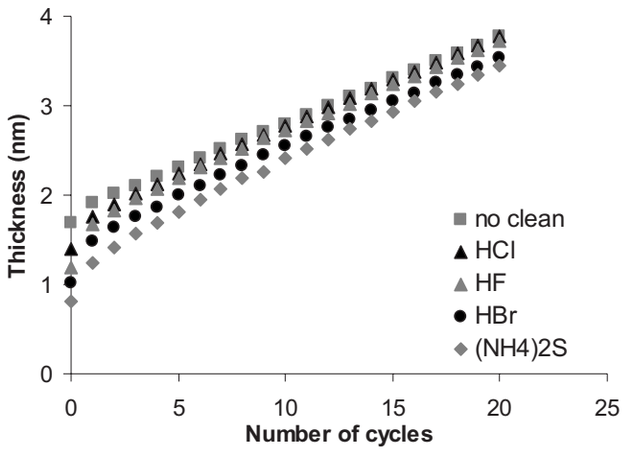

Figure 2. In situ SE measurements during growth of Al_2O_3 by PE ALD. SE measurements are performed after every reaction cycle up to 20 cycles. The slope corresponds to the GPC (nm/cycle). The GPC is independent of the starting surface and is 0.11 ± 0.01 nm.

mined by in situ SE prior to Al_2O_3 deposition. The same trends are observed as by XPS; pretreatments resulting in the lowest oxide content by XPS correspond to the lowest thickness measured by SE. The $(NH_4)_2S$ treatment is only leaving a GaAs oxide of ~0.8 nm compared to the thickness of the no clean of 1.7 nm.

For thermal ALD deposition, only two starting surfaces are considered, no clean and concentrated HCl (37 wt %). XPS data are also shown in Table I and Fig. 1 for both pretreatments. Although XPS data reveal that the concentrated HCl solution more effectively removes oxides, both the concentrated and diluted solution leave some As- and Ga oxides at the surface. In that respect, the pretreatments are comparable, and for simplicity we refer to the HCl clean in this paper for both the diluted and concentrated HCl clean.

Growth per cycle.— In situ SE measurements are shown for the PE ALD deposition in Fig. 2. In situ SE was monitored after deposition of every cycle up to 20 cycles. The model used to characterize the Al_2O_3 deposition has been described by van Hemmen et al.,[15] who showed that SE measurements are able to resolve 1 cycle of Al_2O_3 deposited. All growth curves are linear, and no inhibition is observed. The growth per cycle (GPC) for all pretreatments is 0.11 ± 0.01 nm. We can conclude from these results that the pretreatment has no influence on the growth curve. As all pretreatments result in the same growth behavior, two pretreatments are chosen for further studying the PE ALD process: $(NH_4)_2S$ and HCl.

In Fig. 3 and 4, we present the growth curves for both thermal ALD and PE ALD based on TXRF and ex situ SE measurements. TXRF was measured on samples with various amounts of Al_2O_3 up to 20 cycles, while SE growth curves are determined for films up to 10 nm (~100 cycles). TXRF is not able to measure thick films, as saturation levels off the values measured for thick films. However, both techniques show the same trend; PE ALD deposition of Al_2O_3 on GaAs results in a higher GPC independent of the surface treatment. The GPC for PE ALD is ~0.11 nm (4 Al/nm^2), while the GPC for thermal ALD is ~0.09 nm (3 Al/nm^2). We can conclude that a more reactive oxidant leads to a higher GPC.[15]

The TXRF results show that for all conditions, we have an enhancement in the first cycle (Al content is ~7 to 10 Al/nm^2). With SE it is difficult to distinguish between enhancement in the first cycle and growth of the interfacial oxide when using a two-layer model. However, TXRF is detecting the Al content. Therefore, TXRF provides direct evidence for enhancement in the first cycle. Similar GPC values were found for thermal ALD of HfO_2 by HCl_4/H_2O process on Ge substrates.[20] A steady-state growth is reached after 20 cycles and is ~4 Al/nm^2 for PE ALD. However,

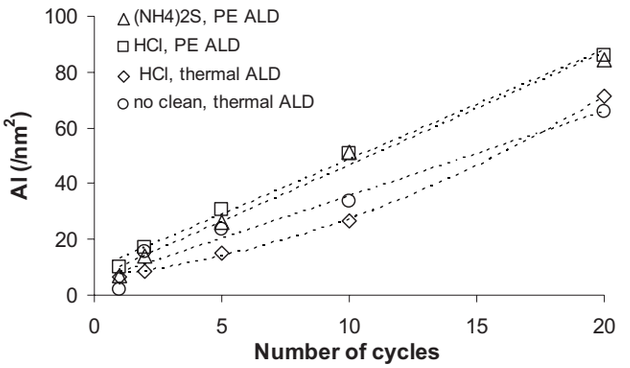

Figure 3. Al content as a function of cycles deposited, determined by TXRF. The symbols represent the measured data points. The dashed lines serve as a guide for the eye.

for the thermal ALD process on HCl-cleaned samples, we see that after the first cycle, which is enhanced, the growth is slightly inhibited in the subsequent cycles. As a result, there is a minor difference upon surface pretreatment in the case of the thermal ALD process. The same effect was observed for thermal ALD HfO_2 deposition on GaAs.[21] However, for the HfO_2 ALD, the difference between the untreated substrate and the HCl-cleaned substrate was more pronounced. It was shown that the HfO_2 ALD proceeded by an island-growth mechanism due to removal of reactive sites by the HCl clean. The reactivity of the Al_2O_3 precursor is probably higher, which explains why the influence of the surface pretreatment is fading in comparison with the HfO_2 growth.

Interfacial layer.— In Fig. 5, an overlay plot of the XPS spectra of the As 3d and Ga 3d peaks are presented for the GaAs substrates before and after deposition of 20 cycles of Al_2O_3 with PE ALD. All spectra are measured at an angle of 28.88°, which is not surface sensitive and is able to detect the interfacial oxides present. AR (angle resolved)-XPS spectra (not shown) were taken. The spectra showed that the signal of the As and Ga oxides is arising from the interface between the GaAs substrate and the Al_2O_3 layer. In Fig. 5, it can be seen that As 3d and Ga 3d spectra after deposition look similar for substrates with different pretreatments. After deposition, the peak becomes larger and broader. As^{3+} increases, and the peak shift to higher binding energy indicates the formation of As^{5+} during PE ALD deposition. The Ga 3d spectra follow the same trend; the Ga oxides after deposition are comparable to the no-clean sample

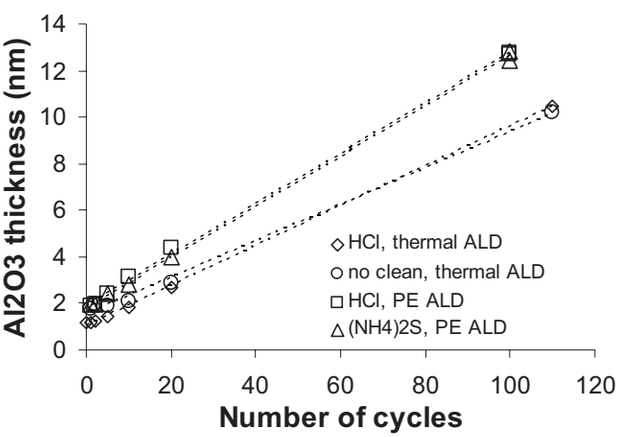

Figure 4. Thickness of Al_2O_3 as a function of cycles measured by ex situ SE. The symbols represent measured data points, and the dashed lines represent fitted curves.

Downloaded 11 May 2009 to 131.155.151.77. Redistribution subject to ECS license or copyright; see http://www.ecsdl.org/terms_use.jsp

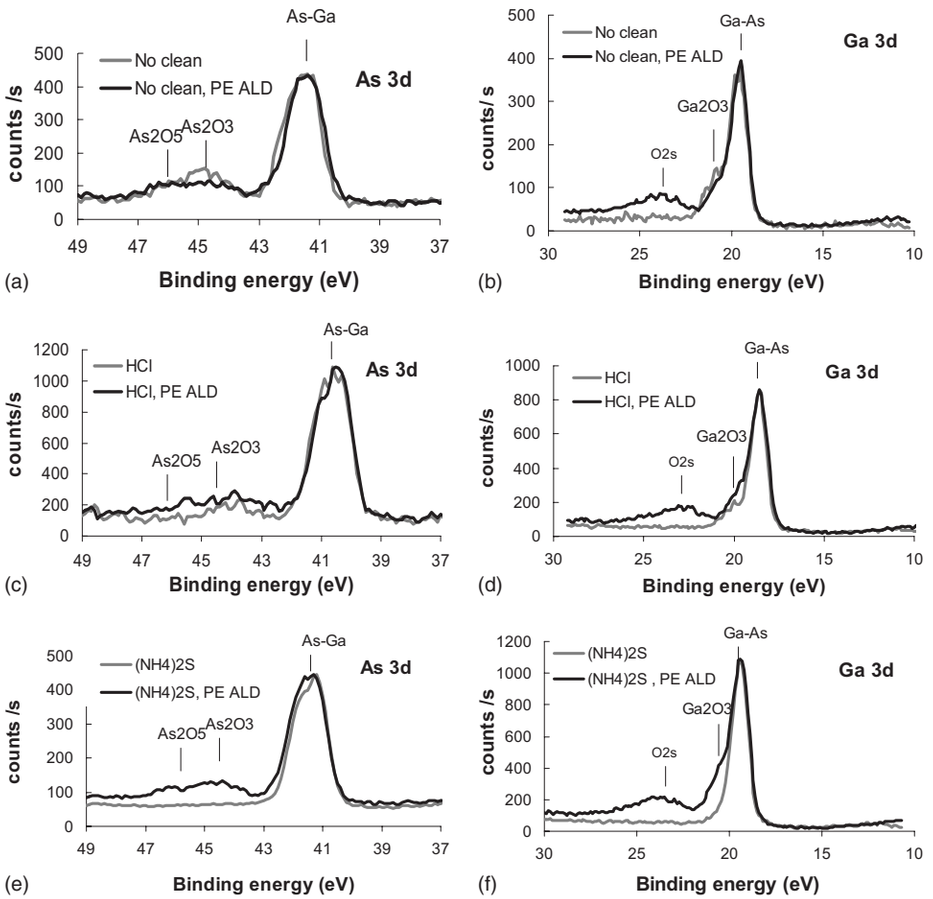

Figure 5. Overlay plot for XPS data of the As 3d and Ga 3d for the GaAs substrate before and after deposition of 20 cycles of PE ALD Al_2O_3: (a and b) the untreated sample, (c and d) the HCl-cleaned sample, and (e and f) the $(NH_4)_2S$-treated sample.

and are independent of the surface pretreatment. In the Starting surface section, it was clear that the $(NH_4)_2S$ treatment was most effective in removing the native oxides present, followed by the HCl clean. After PE ALD, the amount of interfacial oxides is independent of the pretreatment.

In Fig. 6, an overlay of the As 3d and Ga 3d spectra is shown for the GaAs substrate before and after deposition of 20 cycles of Al_2O_3 by thermal ALD. Here we see a striking difference between PE ALD and thermal ALD. In contrast to PE ALD, the thermal ALD process thins the oxide peak for both As and Ga oxides. Moreover, the thinning is more efficient for a starting surface with less residual native oxides (HCl cleaned). After fitting, it is clear that the HCl-cleaned sample contains no As oxides after deposition, while for the uncleaned sample some As oxides are still present. This interfacial self-cleaning effect with thermal ALD on GaAs has already been reported in literature.[9,10,22,23] The TMA precursor is reactive and reduces As oxides in favor of Al_2O_3 formation. However, in the case of PE ALD, the strong O_2 plasma oxidizes the remaining As to As^{5+}. For the thermal ALD process, H_2O is not able to oxidize the remaining As.

Another way to study the interfacial layer after deposition is to use the growth curves determined by ellipsometry. In Fig. 4, the growth curves are presented for PE ALD and thermal ALD. The data shown in Fig. 4 are all extracted from ex situ measurements. This means that the two-layer model is used in this case and that the interfacial oxide is included in the Al_2O_3 layer. When plotting the thickness of the Al_2O_3 as a function of the number of cycles, the intercept is an indication of the interfacial oxide after deposition. In the Growth per cycle section, we could conclude that the PE ALD growth was independent on the starting surface, but extraction of the interfacial layer from the intercept shows that the interfacial thickness depends on the initial thickness of the GaAs oxide (see also Table I). However, none of the treatments are able to prevent oxidation of the interface and the differences in interfacial oxide thickness are minor after the PE ALD Al_2O_3 deposition. The cleaning chemistry that is most effective in preventing reoxidation is the $(NH_4)_2S$ treatment.

From Fig. 4, a comparison can be made between PE ALD and thermal ALD. Clearly, the growth of the interfacial oxide is larger on PE ALD than for thermal ALD. For PE ALD, the thickness of the interface is 1.92 and 1.8 nm for HCl and $(NH_4)_2S$ treatment, respectively. The thermal ALD process results in lower interfacial thicknesses of 1.06 nm for the HCl-cleaned surface and 1.55 nm for the uncleaned surface. Also, we observe a more pronounced difference upon the cleaning chemistry. The uncleaned sample results in a thicker interfacial oxide. From ellipsometry measurements we can conclude that the interfacial oxide after PE ALD is slightly dependent on the surface pretreatment and the oxide is growing during the deposition process. In contrast, the interfacial oxide is thinner after thermal ALD, and a more pronounced difference on the surface pretreatment is observed. Although surface pretreatments play a role in reoxidation of the interfacial oxide, the reactivity of the Al_2O_3 precursors is more important. The O_2 plasma oxidizes the interface more readily than the H_2O pulse for the thermal ALD process, and TMA reduces the GaAs oxide when it reacts with the surface, as shown for the HCl-cleaned thermal ALD process.

Growth mode.— A technique used to determine the growth mode is TOF-SIMS. For ideal 2D growth, the substrate intensity should decay exponentially. However, from TOF-SIMS depth profiles, it was clear that the GaAs substrate intermixes with the Al_2O_3 layer. In such a case, the substrate intensity decays slower, and the technique is thus no longer suitable for determination of the growth mode. In Fig. 7, the depth profiles are given for 10 nm Al_2O_3 layers deposited

Downloaded 11 May 2009 to 131.155.151.77. Redistribution subject to ECS license or copyright; see http://www.ecsdl.org/terms_use.jsp

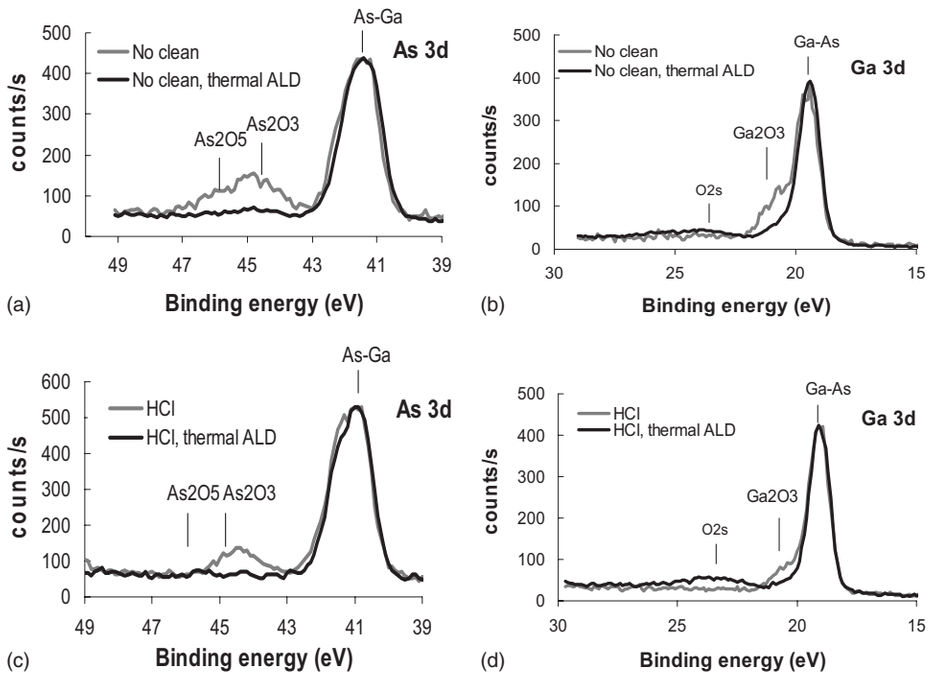

Figure 6. Overlay plot for XPS data of the As 3d and Ga 3d for the GaAs substrate before and after deposition of 20 cycles of thermal ALD Al_2O_3: (a and b) the untreated sample and (c and d) the HCl-cleaned sample.

by thermal ALD. The depth profiles for PE ALD layers are not shown, but the profiles look similar. As, Ga, and Al signals are shown, and it is clear that intermixing of Al_2O_3 with the substrate occurs. From Fig. 7, we can see that we have a diffusion-like profile for the Ga signal in the Al_2O_3 layer with a diffusion length of ~5 nm. HfO_2 films deposited by thermal ALD on GaAs substrates have been shown to lead to a much sharper interface compared to the Al_2O_3 films.[24]

However, some information on the growth mode can be extracted from the XPS data. For PE ALD growth, no inhibition was detected, and a 2D growth can be assumed with fast layer closure. Thermal ALD on a HCl-cleaned GaAs substrate shows a slightly inhibited growth in the first cycles. This could result in slow layer closure. During thermal ALD, the oxide at the interface is consumed by the ALD reaction. As a result, the XPS spectra immediately after deposition show no or small amounts of As- and Ga oxides in the As 3d and Ga 3d spectra, respectively. If the layer is not closed, these oxides could regrow, and a measurement of the same samples after 1 week would show a higher content of As- and Ga oxides. As can be seen in Fig. 8, the As oxides in the XPS spectra did not change after a week for the thermally grown ALD layers on both an uncleaned and a HCl-cleaned GaAs substrate. This is an indication that both layers are closed. Although the growth curves show a minor inhibition, a 2 nm thermal ALD layer on a HCl-cleaned GaAs substrate is closed.

Contamination at the interface.— TOF-SIMS can also be used to determine the contamination incorporated in the Al_2O_3 layer during deposition (see Fig. 9). A depth profile has been taken for samples with 100 cycles of PE ALD Al_2O_3 (~10 nm) and 110 cycles of thermal ALD Al_2O_3 (~10 nm). For all the uncleaned samples, Si contamination is found at the interface independent of the type of ALD process. For C, CN, and S contamination, a remarkable result is found (see Fig. 9a and b). Both uncleaned samples show this contamination at the interface. However, the amount for the PE ALD process is much smaller by a factor of 2–4. This indicates that the contamination present at the surface is oxidized, resulting in volatile compounds of C–O, N–O, and S–O, which are removed from the interface. In the case of the samples treated with $(NH_4)_2S$, S is still present at the interface, although the deposition process is PE ALD. However, the S present before deposition is on the order of 1 monolayer and is 2 orders of magnitude higher than for the uncleaned samples. Moreover, the S is not physisorbed to the surface but probably chemically bonded to the GaAs substrate, which makes it more difficult to remove the S passivation layer from the interface.

Cl was found at the interface of several samples (see Fig. 9c). Similar to the Si samples, a Cl background level is always found on GaAs samples due to cross-contamination from the clean-room environment. Both HCl-cleaned samples contain Cl at the interface. However, for the PE ALD, besides the peak at the interface, the Cl is also diffusing into the Al_2O_3. In contrast, with the thermal ALD process, the Cl stays at the interface. Also, for the uncleaned samples, Cl is detected, and here the same observations are made as for the C, CN, and S contamination; after PE ALD, the Cl contamination is much smaller than for the thermal ALD process.

F was only intentionally introduced for the HF-treated sample followed by PE ALD deposition (see Fig. 9d). Remarkably, for both thermal ALD processes, F is present at the same level as for the HF-treated sample and is incorporated throughout the whole Al_2O_3 layer. The F present on these two samples could be due to cross-contamination occurring during sample handling. On the other

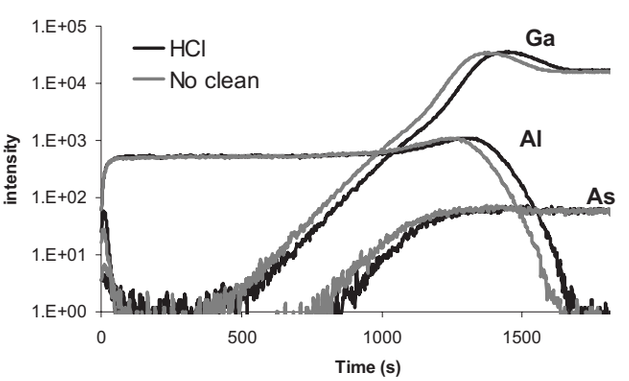

Figure 7. As, Ga, and Al profiles for 10 nm thick Al_2O_3 layers deposited by thermal ALD. Uncleaned and HCl-cleaned substrates are presented.

Downloaded 11 May 2009 to 131.155.151.77. Redistribution subject to ECS license or copyright; see http://www.ecsdl.org/terms_use.jsp

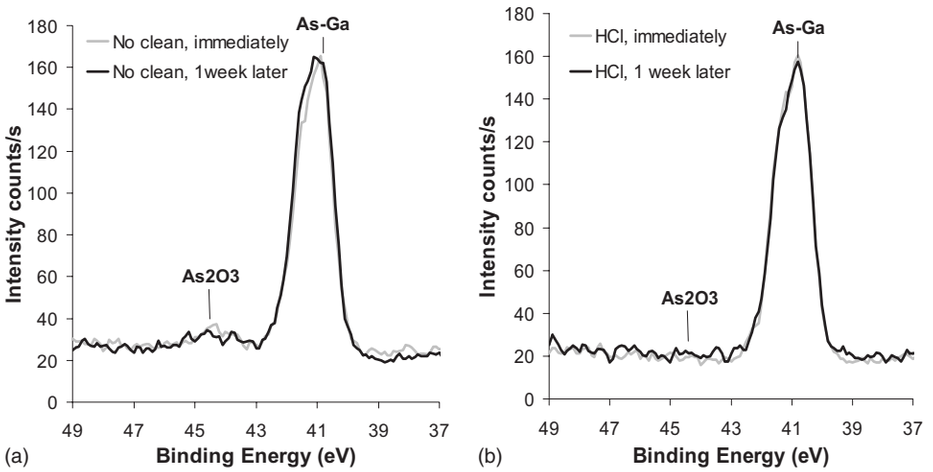

Figure 8. XPS spectra of the As 3d peak immediately after deposition and 1 week later: (a) uncleaned GaAs with 2 nm thermal ALD Al_2O_3 layer and (b) HCl-cleaned GaAs with 2 nm thermal ALD Al_2O_3 layer.

samples, a background of F is detected. However, as TOF-SIMS is sensitive to F, a background of F is always detected.

Br is present at the interface of the HBr-treated sample, and trace amounts are also found for some H*X* (*X* = F, Cl, Br)-treated samples, as Br is a trace element in these H*X* solutions. $(NH_4)_2S$-treated samples show a high amount of several elements at the interface: Mg, Mn, Ca, K, and Na. After PE ALD, these elements are still present, as their oxides are thermally stable. The influence on electrical characteristics of these metals is not yet clear. Although one monolayer of S is present which is known for passivating the interface, an improvement on the electrical characteristics is not shown for the PE ALD Al_2O_3 (see the Electrical characterization section).

We can conclude from the TOF-SIMS results that PE ALD is able to remove several contaminants from the interface with high-*k* due to the oxidizing power of the O_2 plasma, which transforms the contaminants in volatile compounds. This results in cleaner interfaces.

Roughness of deposited layers.— AFM results are summarized in Table II for 10 nm thick Al_2O_3 layers. As can be seen from the data, all samples show good roughness values. Moreover, the values are all in the same order of magnitude. A slightly higher root-mean-square (rms) value is detected for the HCl-cleaned sample with thermally deposited Al_2O_3, which would confirm an island-growth mechanism, resulting in rougher surface. However, the effect is almost negligible.

Electrical characterization.— The results of quasi-static measurements are presented in Fig. 10. Knowing that the midgap interface traps have long time constants,[25] we used a slow voltage sweep

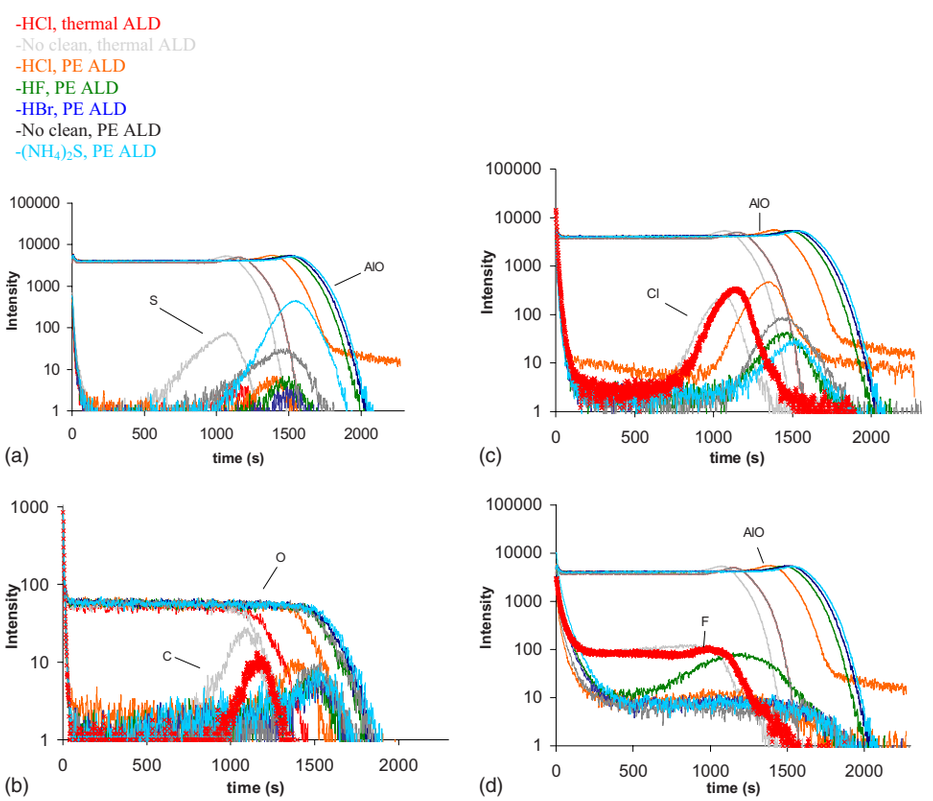

Figure 9. (Color online) TOF-SIMS negative depth profiles: (a) depth profile for S atoms and AlO atoms, (b) for C and O atoms, (c) for Cl and AlO atoms, and (d) for F and AlO atoms.

Downloaded 11 May 2009 to 131.155.151.77. Redistribution subject to ECS license or copyright; see http://www.ecsdl.org/terms_use.jsp

Table II. AFM data for a 2 × 2 μm scan area for 10 nm Al_2O_3 layers on GaAs.

	RMS (nm) of 2 × 2 μm	R_a (nm) of 2 × 2 μm
No clean, thermal ALD	0.208	0.161
HCl, thermal ALD	0.216	0.167
No clean, PE ALD	0.215	0.164
HCl, PE ALD	0.206	0.159
HF, PE ALD	0.198	0.157
HBr, PE ALD	0.199	0.158
$(NH_4)_2S$, PE ALD	0.203	0.161

rate of 3 mV/s for the quasi-static *C-V* measurements in order to assure that the measurement is done in equilibrium conditions. The expression $1 - (C/C_{OX})$, which is equal to the derivative of surface potential with respect to the applied bias under the condition of thermal equilibrium, is plotted in Fig. 10a. One can see a clear difference in the amount of surface-potential change with applied bias voltage between PE ALD samples and thermal ALD samples. Calculating the Berglund integral,[16] we can show that the surface-potential variation is ~0.4 eV in the case of PE ALD and ~0.6 eV in the case of thermal ALD. Both values are nevertheless substantially smaller than the GaAs bandgap, and we can conclude that in both cases the Fermi level is not free to move over the whole bandgap.

In order to confirm the hypothesis that thermal ALD results in better interface quality, further investigation of the HCl-cleaned samples was performed. As can be seen in Fig. 10b, the thermal ALD sample shows less hysteresis, which indicates a lower density of slow states at the GaAs-oxide interface. Moreover, the two samples have different frequency dispersion of accumulation capacitance. As presented in Fig. 10c, the thermal ALD sample shows about 5% variation of accumulation capacitance for frequencies varying from 1 to 100 kHz, whereas there is about 10% variation for the PE ALD sample. The sudden increase in frequency dispersion at frequencies larger than 100 kHz can be attributed to series resistance, because it changes with the size of the device under test.[17] This amount of frequency dispersion observed is similar to other published results,[12,26-30] although it is difficult to compare, as most research groups do not publish this data in detail. Also, the surface-potential variation at the GaAs-oxide interface is not generally reported in literature. More detailed information about CV characterization of GaAs MOS can be found in Ref. 31.

The electrical measurements show that samples prepared by thermal ALD demonstrate larger movement of the Fermi level at the surface. Also, they demonstrate less frequency dispersion and lower hysteresis in the *C-V* curves. The better results of the thermal ALD samples are probably related to thinning of the interfacial oxide with removal of As oxides. Nevertheless, the movement of the surface potential is considerably less than the GaAs bandgap, which shows that the Fermi level is not free to move over the entire GaAs bandgap, and more research is still needed to passivate the interface prior to high-*k* deposition.

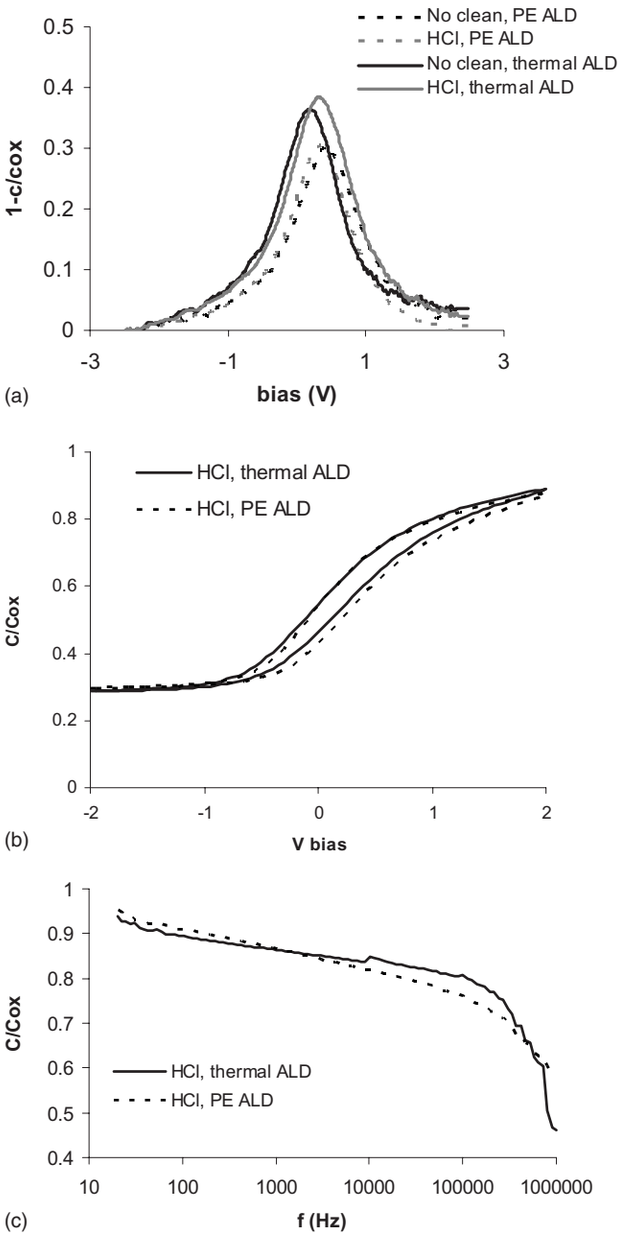

Figure 10. (a) Experimentally obtained derivative of surface potential with respect to the applied voltage. (b) *C-V* curves taken at 1 kHz. (c) Frequency dispersion of the capacitance measured in accumulation.

Conclusions

PE and thermal ALD deposition of Al_2O_3 on GaAs was studied, and a comparison was made for both deposition techniques. In addition, the influence of the starting surface was studied using several chemical treatments prior to deposition.

To qualify the high-*k* layer, several techniques have been used, and an electrical characterization of the ALD layers has been carried out. PE ALD shows that a more reactive precursor makes the growth independent of the pretreatment; it is a linear growth with enhancement in the first cycle. During PE ALD, the interface is oxidized, and the thicker the starting oxide, the thicker the interfacial layer after deposition. As^{3+} and As^{5+} are present. Because of the high oxidizing power, this process is able to clean C, S, and CN impurities at the starting surface during deposition. In contrast, thermal ALD deposition shows differences upon surface pretreatment. Also, for this deposition process, a linear growth with enhancement in the first reaction cycle is observed. A small inhibition effect is seen for the HCl-cleaned surface, possibly related to island formation during the first cycles. Compared to PE ALD, the steady GPC of the thermal ALD process is smaller. However, during deposition a thinning of the interfacial oxide is observed. As oxides are completely removed, and Ga oxides are reduced. However, more contaminants (C, CN, S) are detected at the interface.

The ALD layers were also electrically qualified, and better CV characteristics (less hysteresis, frequency dispersion, and larger movement of the surface potential) were observed for the thermal ALD layers. At this stage, we can assume that the better electrical

Downloaded 11 May 2009 to 131.155.151.77. Redistribution subject to ECS license or copyright; see http://www.ecsdl.org/terms_use.jsp

characteristics of the thermal ALD layers is related to the thinning of the interface. Although removal of contaminants at the interface can play an important role, this could also be achieved in thermal ALD by choosing the appropriate pretreatment. However, both thermal as well as PE ALD layers show both severe problems regarding the electrical characteristics. The Fermi level is still pinned, as shown by the amount of surface-potential movement at the GaAs-oxide interface (0.6 eV in the best case), which is considerably smaller than the GaAs bandgap. Therefore, more research is needed to passivate the interface.

Acknowledgments

The authors acknowledge support by the European Commission's project FP7-ICT-DUALLOGIC no. 214579 "Dual-channel CMOS for (sub)-22 nm high performance logic."

IMEC assisted in meeting the publication costs of this article.

References

1. G. Nicholas, B. De Jaeger, P. Zimmerman, D. P. Brunco, B. Kazcer, G. Eneman, M. Meuris, and M. M. Heyns, Institute of Scientific and Technical Communicators, West Sussex, UK, Oct 3-5, 2006.
2. M. Green, M.-Y. Ho, B. Bush, G. D. Wilk, T. Sorsch, T. Conard, B. Brijs, W. Vandervorst, P. I. Raisanen, D. Muller, et al., *J. Appl. Phys.*, **92**, 7168 (2002).
3. M. A. Alam and M. L. Green, *J. Appl. Phys.*, **94**, 3403 (2003).
4. N. Nyns, L. Hall, T. Conard, A. Delabie, W. Deweerd, M. Heyns, S. Van Elshocht, N. Van Hoornick, C. Vinckier, and S. De Gendt, *J. Electrochem. Soc.*, **153**, F205 (2006).
5. R. L. Puurunen, *Chem. Vap. Deposition*, **9**, 249 (2003).
6. R. L. Puurunen, *J. Appl. Phys.*, **95**, 4777 (2004).
7. T. Conard, W. Vandervorst, J. Petry, C. Zhao, W. Besling, H. Nohira, and O. Richard, *Appl. Surf. Sci.*, **400**, 203 (2003).
8. E. P. Gusev, C. Cabral, Jr., M. Copel, C. D'Emic, and M. Gribelyuk, *Microelectron. Eng.*, **69**, 145 (2003).
9. P. D. Kirsch, M. A. Quevedo-Lopez, H.-J. Li, Y. Senzaki, J. J. Peterson, S. C. Song, S. A. Krishnan, N. Moumen, J. Barnett, G. Bersuker, et al., *J. Appl. Phys.*, **99**, 023508 (2006).
10. M. L. Huang, Y. C. Chang, C. H. Chang, Y. J. Lee, and P. Chang, *Appl. Phys. Lett.*, **87**, 252104 (2005).
11. M. L. Huang, Y. C. Chang, C. H. Chang, and T. D. Lind, *Appl. Phys. Lett.*, **89**, 012903 (2006).
12. Y. Xuan, H. C. Lin, P. D. Ye, and G. D. Wilk, *Appl. Phys. Lett.*, **88**, 263518 (2006).
13. R. Puurunen, *J. Appl. Phys.*, **97**, 121301 (2005).
14. P. R. Lefebvre and E. A. Irene, *J. Vac. Sci. Technol. B*, **15**, 1173 (1997).
15. J. L. van Hemmen, S. B. S. Heil, J. H. Klootwijk, F. Roozeboom, C. J. Hodson, M. C. M. van de Sanden, and W. M. M. Kessels, *J. Electrochem. Soc.*, **154**, G165 (2007).
16. C. N. Berglund, *IEEE Trans. Electron Devices*, **13**, 701 (1966).
17. K. Martens, W. Wang, K. De Keersmaecker, G. Borghs, G. Groeseneken, and H. Maes, *Microelectron. Eng.*, **84**, 2146 (2007).
18. S. Arabasz, E. Bergignat, G. Hollinger, and J. Szuber, *Vacuum*, **80**, 888 (2006).
19. J. Shin, K. M. Geib, C. W. Wilmsen, and Z. Lilliental-Weber, *J. Vac. Sci. Technol. A*, **8**, 1894 (1990).
20. A. Delabie, R. L. Puurunen, B. Brijs, M. Caymax, T. Conard, B. Onsia, O. Richard, W. Vandervorst, C. Zhao, M. M. Heyns, et al., *J. Appl. Phys.*, **97**, 064104 (2005).
21. A. Delabie, L. Nyns, M. Caymax, T. Conard, A. Franquet, M. Houssa, D. Lin, M. Meuris, L.-A. Ragnarsson, S. Sioncke, et al., *ECS Trans.*, **11**(7), 227 (2007).
22. C. L. Hinkle, A. M. Sonnet, E. M. Vogel, S. McDonnell, G. J. Hughes, M. Milojevic, B. Lee, F. S. Aguirre-Tostado, K. J. Choi, H. C. Kim, et al., *Appl. Phys. Lett.*, **92**, 071901 (2008).
23. M. Frank, G. D. Wilk, D. Starodub, T. Gustafsson, E. Garfunkel, Y. Chabal, J. Grazul, and D. A. Muller, *Appl. Phys. Lett.*, **86**, 152904 (2005).
24. A. Delabie, D. P. Brunco, T. Conard, P. Favia, H. Bender, A. Franquet, S. Sioncke, W. Vandervorst, S. Van Elshocht, M. M. Heyns, et al., *J. Electrochem. Soc.*, **155**, H937 (2008).
25. G. Brammertz, K. Martens, S. Sioncke, A. Delabie, M. Caymax, M. Meuris, and M. M. Heyns, *Appl. Phys. Lett.*, **91**, 133510 (2007).
26. D. Shahrjerdi, E. Tutuc, and S. K. Banerjee, *Appl. Phys. Lett.*, **91**, 063501 (2007).
27. H.-S. Kim, I. Ok, M. Zhang, F. Zhu, S. Park, J. Yum, H. Zhao, and J. C. Lee, *Appl. Phys. Lett.*, **91**, 042904 (2007).
28. K. Dalapati, Y. Tong, W. Y. Loh, H. K. Mun, and B. J. Cho, *Appl. Phys. Lett.*, **90**, 183510 (2007).
29. I. Ok, H. Kim, M. Zhang, F. Zhu, S. Park, J. Yum, H. Zhao, and J. C. Lee, *Appl. Phys. Lett.*, **91**, 132104 (2007).
30. D. Choi, E. Kim, P. C. McIntyre, and J. S. Harris, *Appl. Phys. Lett.*, **92**, 203502 (2008).
31. G. Brammertz, H. C. Lin, K. Martens, D. Mercier, C. Merckling, J. Penaud, C. Adelmann, S. Sioncke, W. E. Wang, M. Caymax, et al., *J. Electrochem. Soc.*, **155**, H945 (2008).

Downloaded 11 May 2009 to 131.155.151.77. Redistribution subject to ECS license or copyright; see http://www.ecsdl.org/terms_use.jsp